MSc in Photonics

PHOTONICS**BCN**

Universitat Politècnica de Catalunya (UPC)
Universitat Autònoma de Barcelona (UAB)
Universitat de Barcelona (UB)
Institut de Ciències Fotòniques (ICFO)

http://www.photonicsbcn.eu

Master in Photonics

MASTER THESIS

Ultra short laser pulse characterization device based on disordered nonlinear crystals

Guillermo Cubero Gamito

Supervised by Dr. Jose Trull (UPC)
and Dr. Crina Cojocaru (UPC)

Presented on date 27th October 2017

Registered at

Escola Tècnica Superior d'Enginyeria de Telecomunicació de Barcelona

Ultra short laser pulse characterization device based on disordered nonlinear crystals

Guillermo Cubero Gamito
Grupo de Dinámica y Óptica No Lineal y Láseres (DONLL)
Departamento de física
Universitat Politècnica de Catalunya
Rambla Sant Nebridi 22, 08222, Terrassa,Barcelona - SPAIN
E-mail: cubero@gmail.com
October 2017

Abstract

In this project we build and test a compact and portable optical device for ultrashort pulse characterization. This setup allows the measurement of the pulse duration as well as its chirp parameter by using the so called transverse single-shot auto-correlation scheme, using, as novelty, a random nonlinear crystal. A companion software has been developed to automatize the device and process the acquired data by following a preprogrammed algorithms and showing the results in easy and understandable manner.

Keywords: nonlinear optics, short pulse measurements, photonic crystals

INTRODUCTION

The interaction of the light with matter strongly depend on the light intensity. Ultrashort laser pulses in femtosecond (fs) regime are nowadays an essential tool in a wide range of applications, both in science as well as in technology. Material processing, laser micromachining, optical communications, high-resolution imaging and detection, investigation of complex molecular system's dynamics, biophotonics and medical science, are only few examples of such applications. These applications are meaningful only if one is able to precisely characterize the laser pulses used in the experiment. With the same amount of mean energy emitted by a pulsed laser, the shorter the pulse is, the higher is its intensity. Therefore, only knowing with precision the temporal duration as well as its spatial distribution let us determine with precision the pulse intensity in terms of W/cm^2, and so the strength of its interaction with matter

There are several methods to partially or completely characterize a laser pulse. When the pulse duration is bellow ns scale electronic direct measurement are not fast enough and only indirect methods,

most of them based on nonlinear optical interactions, can be used. Some of these techniques are based on a cross-correlation setup, (such as the so called FROG [7,8]), where the pulse to be measured is mixed with another well known reference pulse. The reference pulse act as an optical gating recording the pulse profile by using a multi-shot experiment where the reference pulse is intentionally delayed in front the other to perform an interaction along the whole unknown pulse duration. Another possibility is to use an auto-correlation technique, where the optical gating is done by overlapping the pulse to be measured with its own replica. Some of these techniques allow an extensive characterization of the pulse, measuring all its parameters. Others make a partial characterization, measuring only the duration of the pulse.

Both techniques, cross-correlation and auto-correlation, are typically implemented through a nonlinear optical process, as the parametric process of second harmonic generation (SHG). One of the best method for single-shot partial pulse characterization is the non-collinear SHG in where two beams pass through a quadratic nonlinear crystal with a certain angle. It can be demonstrated that the forward generated second harmonic represents the autocorrelation trace of the two overlapped pulses from which we can get the temporal characterization of the pulse.

The SHG conversion performance, defined by equation (1), shows us that if we want to obtain an efficient SH signal we have to minimize the so called phase mismatch factor (Δk), defined in the equation (2).

$$\eta(L)=\frac{I_{2\omega(L)}}{I_{\omega}} \propto \frac{d_{eff}^2 I_{\omega} L^2}{n^2}\frac{\sin^2(\Delta kL/2)}{\Delta kL/2} \tag{1}$$

Where d_{eff} if the nonlinear coefficient, $I\omega$ the intensity of the fundamental beam, n the refractive index, L the length of the nonlinear crystal.

$$\Delta k = 2k^{\omega} - k^{2\omega} \tag{2}$$

where k_{ω} and $k_{2\omega}$ are the wavevectors at the fundamental and at the SH wavelength, respectively.

In this conditions, a second harmonic beam will be generated efficiently if the so called phase matching (PM) condition that states $\Delta k=0$ is fulfilled. For the SHG, for this to happen, both waves, the fundamental and the generated SH, must have the same phase velocity, or, on other works, the material has to be non dispersive ($n_{\omega}=n_{2\omega}$). Unfortunately, this condition as never satisfied by natural materials due to inherent dispersion that makes every frequency travel with different phase velocity

To achieve the phase matching we can use different techniques such as crystal birefringence, quasi phase matching (QPM) technique, or photonic crystals. Those techniques allow to achieve the PM only in a particular propagation direction and for very specific wavelength and require a good degree of precision in the alignment of the crystal or even a temperature tuning. These techniques show a very narrow spectral bandwidth, so they are only usable for a very concrete wavelength. A broader bandwidth can be achieved by using a very thin crystal but it goes against the fact that we need enough material to achieve a proper SHG. This can be a drawback when we want to generate SH from a broadband fundamental beam, as happens when we work with ultrashort pulses: shorter is the pulse, broader is the bandwidth.

QPM structures are based on a periodic engineered materials with a inversion of sign of the nonlinear susceptibility $\chi^{(2)}$ as shown in figure 1a. This change of sign is placed every multiple of the so called coherent length Lc, which is the length over which fundamental and harmonic wave get out of phase.

This condition prevents waves to get out of phase. In the case that fundamental and generated SH are not phase matched we talk about having a phase mismatch that we identify by (2). In a QPM structure obtained by periodically poling a nonlinear crystal we can define a vector defining the spatial periodicity. This vector has a correspondent wave vector in the Fourier domain (reciprocal lattice), called reciprocal lattice vector G, that contributes to that momentum conservation.. To finally reach phase matching condition this reciprocal vector have to compensate the phase mismatch fulfilling the equation (3).

$$\Delta k_{QPM} = \Delta k - G = 0 \qquad (3)$$

As a drawback, those periodically polled materials has to be engineered exclusively for a very concrete frequency and can be adjusted by modifying the incident angle or by thermal tunning.

Few years ago, a novel autocorrelation technique based on the non collinear SHG in a particular type of ferroelectric crystal showing random inverted nonlinear domains has been shown to avoid the bandwidth limitation of the previous techniques [12, 13]. These crystals grow with random-sized nonlinear domains with an inverted sign of the 2nd order susceptibility $\chi^{(2)}$ oriented along the optical axis of the crystal, as seen in figure 1b.

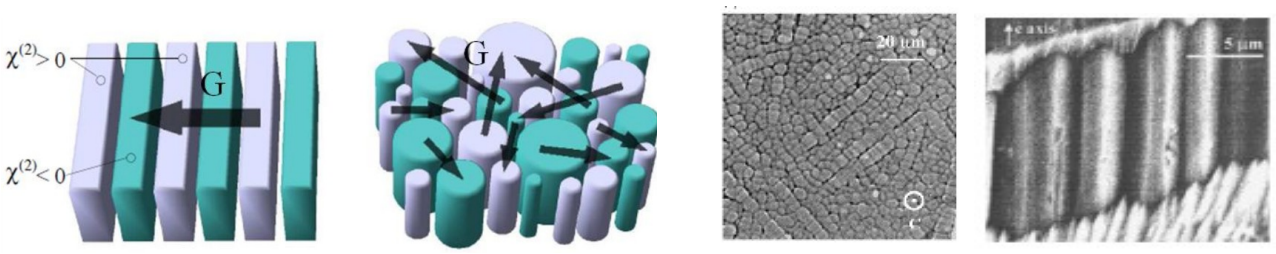

(a) (b) (c) (d)

Fig. 1: a. Strictly periodic structure b. Random-sized nonlinear domain c/d. Random crystal at microscope [10]

The crystal has constant linear refractive index. We can consider this structure as an extension of the QPM technique, but, in this case, instead of having a perfect periodic structure we have a media consisting of anti-parallel nonlinear ferroelectric domains with random sizes and spatial distribution. This random distribution provides an infinite number of reciprocal vectors G or, in other words, provide us phase matching compensation on a spectral broadband and broad angular emission avoiding this narrow spectral band limitations of the QPM. Therefore, phase matching is possible over a broader frequency bandwidth, being limited only by the transparency region of the crystal, and it does not require angular or thermal crystal tuning. As a result, for any fundamental wavevector k_ω of light propagating through the crystal there will be also a matching lattice vector G in this plane to fulfill the phase-matching condition (3). This provide us a media suitable to generate a SH with a phase matching in its whole bandwidth which is convenient for a utra-short pulse characterization due to fact that the shorter the pulse is, the bigger the spectral bandwidth it have. An examples of such disordered nonlinear media are an unpoled Strontium Barium Niobate SBN crystal (SBN) or Calcium Barium Niobate (CBN) with typical domain sizes ranging between 0.1 and 8 μm [9, 10, 11].

Autocorrelation scheme using transverse SHG in a SBN crystal

In this work we implement an as grown SBN crystal, showing the random domain distribution explaimed above, in an autocorrelation scheme between a Gaussian pulse and its replica. The two pulses overlap within the crystal in a non-collinear interaction, propagating in a direction perpendicular to the optical axis of the crystal, as shown in Figure 2a.

This non-collinear interaction produces three well differentiated SH signals in the forward direction as seen in figure 2d. Two of them are emitted as a cone and are due to the SH generated by each input beam independently. Additionally, there is a third central emission that is due to the interaction of both beams and represents the autocorrelation trace which carries the information we need for pulse characterization.

To understand the shape of this central emission, we consider that, as seen in figure 2b, the pulse, with wavevector k^{ω}, and its replica k'^{ω} are propagating on the xz crystallographic plane of the SBN crystal. The distribution and orientation of the random domains produces an infinite set of reciprocal vectors $\vec{G}$, with different modulus and orientation in the xy plane. The generated SH has to fulfill the general PM condition defined by the equation (4):

$$\vec{k}^{2\omega} = \vec{k}^{\omega} + \vec{k}'^{\omega} + \vec{G} \tag{4}$$

Taking into account that these $\vec{G}$ vectors can have any length and direction within this plane, we note that all possible PM triangles determine that the SH radiation is emitted in the form of a whole plane coinciding with the crystal xy plane.

Most autocorrelation techniques that uses nonlinear materials are based on the study of the SH generated in the forward direction. The novelty of our method lies on the fact that, unlike in the other autocorrelations methods, with such random structures we can obtain SH signal generated in a transverse direction with respect to the fundamental beam propagation direction.

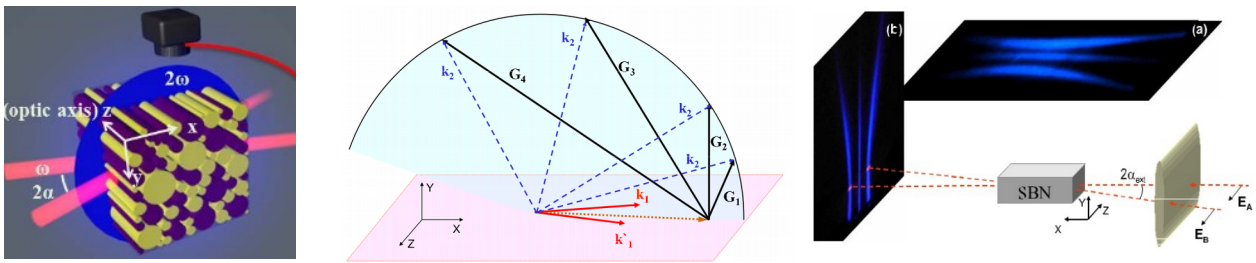

(a) (b) (c)

Fig. 2: (a) Representation of the transverse AC Setup (b) Schematic of the phase-matching diagram of the planar SH emission via interaction of two noncollinear pumps with bisector coinciding with crystal axis X. G_i being the reciprocal vectors of the disordered nonlinear crystal. (c) Schematic presentation of the interacting geometry

The transverse second harmonic generation (TSHG) allow us to place an image sensor on the top of the crystal and to record the transverse SH trace, instead of recording it in the forward direction were we have the original beams as well as the SH ones. As an added benefit, from the top of the crystal we can record the autocorrelation trace evolution along the whole propagation distance within the crystal in a way that the autocorrelation at the entrance is not yet affected by crystal dispersion and, moreover, the

autocorrelation evolution will provide us information about the spectral distribution of the pulse. As we can see in detail in figure 3, as a result of the overlap of the two pulses we obtain this autocorrelation trace from where we can measure the width Δz_{FWHM} of the trace along the crystal. Considering that the pulse has a Gaussian transversal profile, we can obtain a pulse duration τ along the crystal by using the following equivalence:

$$\tau(x)=\frac{\Delta z_{FWHM}(x)\sqrt{2}\sin(\alpha)}{c} \tag{5}$$

Where, Δz_{FWHM} is the transversal full width half maximum and α is the half angle between both replicas of the pulse. The actual input pulse duration would be then $\tau(0)$ calculated at the input of the crystal in where the pulse is not yet affected by the crystal dispersion.

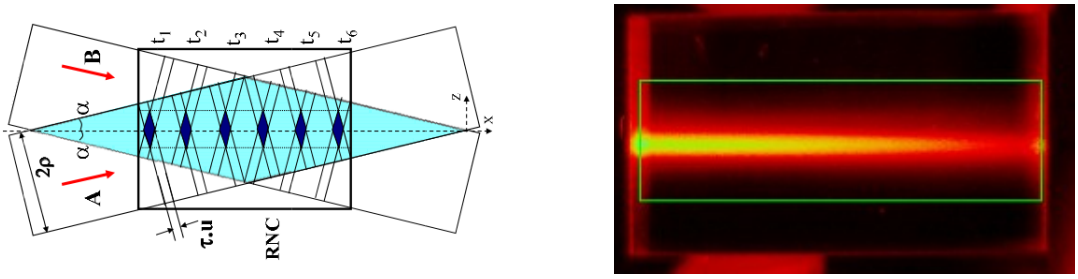

Fig. 3: Non collinear overlap of two beams forming a narrow line inside the crystal viewed from the top

On the other hand, since the fundamental pulse broadens with the propagation distance inside the crystal due to material dispersion, the autocorrelation trace will widen correspondingly as shown in figure 4a. This effect can be used for the chirp characterization of the input femtosecond pulses by using the equation (6), in where C is the chirp expressed in *fs/mm* and g is an dimensionless group velocity dispersion (*GVD*) coefficient. For a negative chirped pulse the equation (6) show us an opposite behavior in where pulse is compressed along the crystal as seen in figure 4b.

$$\tau(x,C)=\sqrt{\frac{4g^2(1+C^2)}{\tau_o^2}x^2+4gCx+\tau_0^2} \tag{6}$$

In those circumstances if the crystal is long enough or the pulse is very short we can see that the pulse duration starts being compressed and after it reaches the shorter pulse possible, the so called Fourier limited pulse, the pulse starts broadening again as shown in figure 4c.

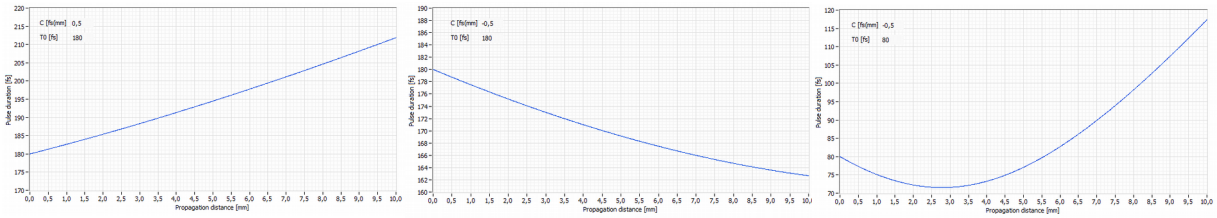

(a) (b) (c)

Fig. 4: Pulse duration evolution inside crystal for (a) positive chirped input pulse. (b) for a negative chirped one (c) for a negative chirped one inside a long crystal

Experimental setup

The implemented setup is schematically shown in figure 5. We first chose the desired laser polarization that has to be set horizontally, along the z axis of the crystal. This polarization gives the most efficient SHG inside the SBN crystal, because it uses the higher component d_{33} of the second order permitivity tensor $\chi^{(2)}$ of the SBN crystal. To do so, we have placed a half wave plate HWP, also known as $\lambda/2$, and a polarizer. A beam splitter BS or also called half mirror splits the pulse in two evenly with the same amount of energy. From now on, both replicas of the pulse follows a different path. The goal is to make both pulses reach the crystal at the same moment and overlap inside the crystal, so they must travel over the same optical path. The upper path, consisting of mirrors M_1, M_2 and M_3 has a fixed length. On the contrary, the lower branch, consisting of M_4, M_5, M_6 and M_7, has variable optical path that has to be adjusted during the experiment until get both pulses to overlap inside the crystal. The variation of this lower branch is made by adjusting the position of the mirrors M_5, M_6 that are placed on a translation stage. Just before the crystal, we have a cylindrical lens. The purpose of this lens is to concentrate the beam, but only in the vertical direction since it is known that nonlinear processes inside crystal occurs only with high enough intensity of light. Finally, the SBN crystal is oriented with its c-axis perpendicular to the axis of the setup and in the plane formed by the input beams.

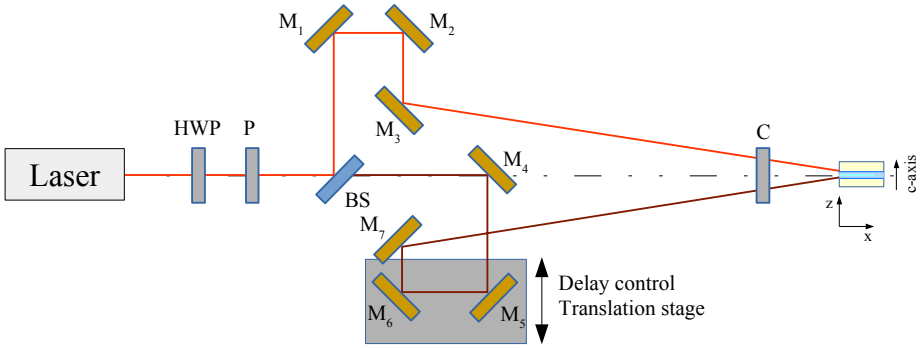

Fig. 5: Setup Schematics of the correlator. P polarizer, M mirror, BS beam splitter, C cylindric lens an HWP Half wave plate or λ/2

One of the requirements of this work was to build a device as compact as possible, trying to maintain it affordable. For that, we have chosen equipment of the brand Optosigma that is established in France but has its roots on Japan. Fortunately, we can find all their products in a digital 3D files from where we have been able to design it very accurately in a 3D software. To do so, we have used the 3D CAD/CAE Software SolidWorks from the French company Dassault Systèmes.

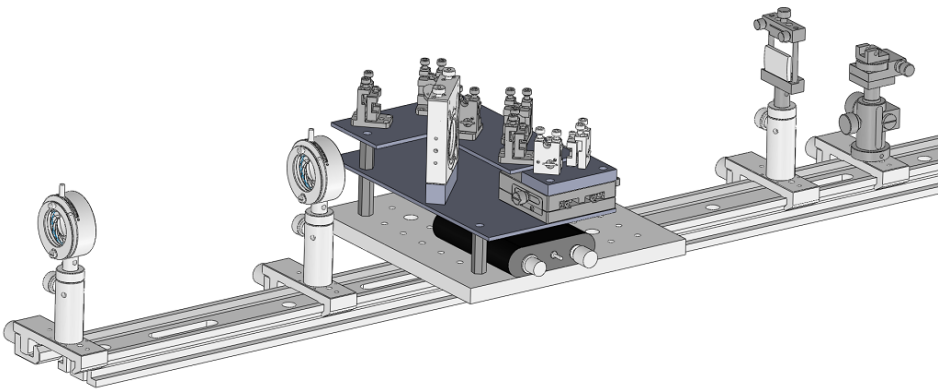

Fig. 6: 3D Model designed with SolidWorks

We have build the system on an extruded aluminum guide where we place all the needed components. Firstly, we have two diaphragms that help us to align the input pulse. This is very critical step because a small misalignment will drive us to an incorrect overlapping of pulses inside the crystal. The distance between them has to be as long as possible to ensure the correct alignment. We have chosen aluminum mirrors with a wide bandwidth ranging from 200nm to 1200nm. This bandwidth is large enough for the application on a femtosecond pulse considering that in this case it have a central wavelength of around 800nm. At the end of the aluminum guide we place the crystal. We have chosen a rotation stage to tune accurately the angle of the crystal. Upon this rotation stage we have designed and build an adapter to hold the crystal firmly by means of a two nylon screws. This adapter is placed in such a way that the rotation center is placed over a facet of the crystal instead of on its center. On the other hand, even having set the polarization before the correlator, the mirrors on the setup can distort it a little bit on every reflexion. To fix this, optionally, between the cylindrical lens and the crystal, we can place a couple half wave plates (λ/2), one for each branch. Regarding to the translation stage, there are several options available on the market. There are those based on a steeper motor which can give us a feedback on the actual position of the translation stage. On the other side, there are a more affordable option based on a direct current (DC) motor. Since our analysis algorithm does not need this position feedback we have chosen this last option. This DC motor is connected to a driver from the same supplier and give us a digital interface to control speed and direction of the translation stage by means of USB connection.

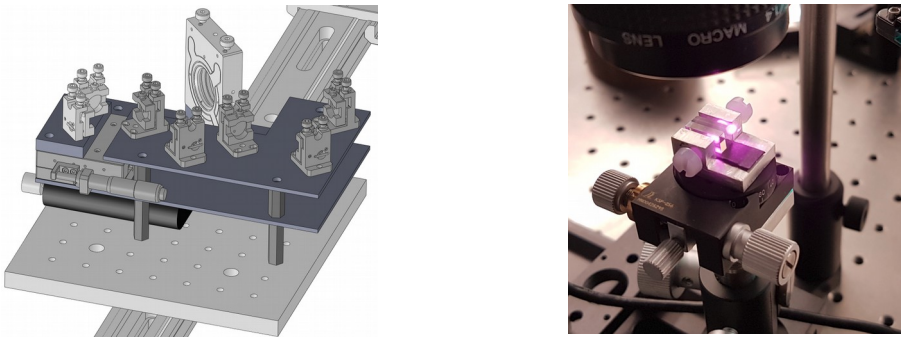

Fig. 7: (a) Correlator consisting in a beam splitter, 7 mirrors and a motorized translation stage (b) Detail of the camera on the top of the crystal fixed with two nylon screws

The are two main option in the market when it comes to beam splitters which are the cubic and the plate. The cubic beam splitter (figure 8a) is not suitable for our setup because introduces too much amount of crystal. This fact, make the pulse travel too much distance inside a dispersive media in a way that it can be broaded or even chirped. This is why we have finally chosen a plate half mirror. Those kind of beam splitters has also the drawback of the double reflection. This second reflection is called ghost beam, and is produced in the second facet of the crystal. To control and minimize the effect of this second beam, we have chosen a wedged half mirror on which, as seen on figure 8b, the two facets are not parallel but they have a certain angle making ghost beam be redirected far from the main beam in such a way that we can control and prevent it to interfere in the rest of the setup.

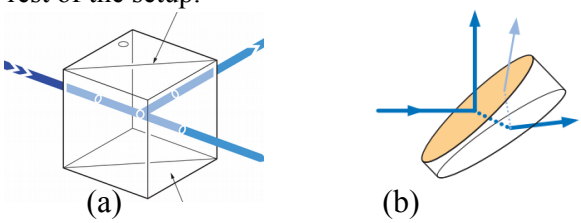

Fig. 8: (a) Cube half mirror. (b) Wedged substrate plate half mirror showing the detail of the ghost beam

Automation and software image processing and results

We have developed a software which automatizes the acquisition process and run a set of algorithms to process the acquired images in a user friendly manner and directly show the results: time duration and chirp parameter. As developing environment we have chosen LabView which is very widespread in the scientific world and allow us to build an easy to use user interface as well as communicate with the acquisition hardware and the translation stage over USB protocol.

Once the image is acquired, we define and implement a calibration tool (figure 9), that defines the region of interest (ROI), with a twofold objective: to define where the second harmonic is generated and, to calibrate the horizontal length of the crystal. Knowing this length the tool automatically calculates the ratio *px/mm*. To be able to do this calibration, several parameters such as beam angle and group velocity dispersion of crystal *g* have to be introduced into the program.

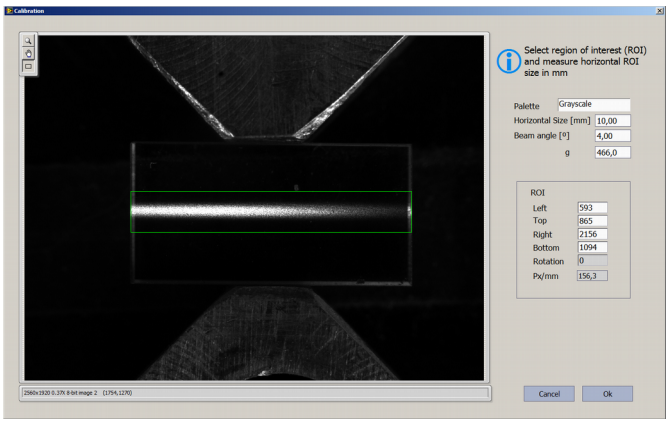

Fig. 9: Calibration dialog

The application begins asking you to press the *set on-line* button. Doing this, the software will start communication with both, translation stage and the camera. Once we have done this, application is ready to start acquisition and analysis. In the meantime we see an on-line image of the SH interaction inside the crystal and the application will let us move the translation stage freely. In addition, there is a search algorithm implemented called *sweep,* which will search along the whole translation stage travel looking for the very position in where the beams overlaps inside the crystal. Using this function, the translation stage goes to its origin, and moves along its whole rank until a SH interaction is seen on the image.

At this point we realize that images are pretty noisy so we must follow some strategy in order to clean up the acquired images without losing information. We start by recording and combining three images from the same position of the translation stage. Afterwards, we use a space domain filter to average every pixel with their neighborhood. Finally, we filter column by column, using an average filter in order to obtain an almost noiseless Gaussian profile on every column.

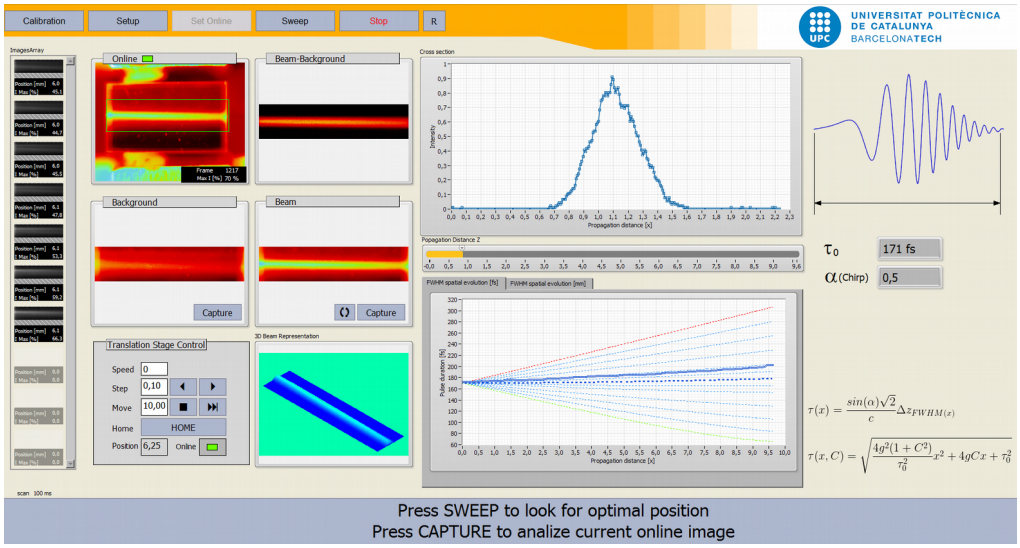

Fig. 10: Main application dialog

Once we have the image ready, we start the analysis. First, it is computed the width at half maximum ΔZ_{FWHM} of the Gaussian profile by using an insensitive to the noise algorithm. This algorithm computes the integral of the Gaussian profile and check where this integral gets the 14% and 86% of the total area. The distance between those percentages are equivalent to the ΔZ_{FWHM} of a Gaussian beam. If the shape of the beam is different to a Gaussian we would need to use other values for the integral.

Having calculated the ΔZ_{FWHM} of the generated SH along the crystal the application continues by applying the equation (5) from where we get a curve of τ along the crystal. The first value $\tau(0)$ is the pulse duration at the crystal entrance and represents the actual pulse duration. The evolution of ΔZ_{FWHM} along the crystal, whether it is growing or getting narrower, indicates in some way that the pulse has chirp. Positive chirped pulse shows a growing SH width evolution and, on the contrary, negative chirped pulse shows a narrowing SH width evolution. To find out the actual chirp of the analyzed pulse the curve is compared with a set of precalculated curves for a various values of chirp by mean of the equation (6). The application, finally, compares the actual curve with every chirp curve and deduces which is the most suitable one.

The experimental setup has been tested using a pulsed Ti:Sapphire laser with a FWHM duration of 180 fs with a central wavelength of 800 nm and with energies of 20 nJ/pulse. The setup was adjusted with a half angle between both replicas of the pulse of 6º. The image sensor was a color camera μEye IDS-1250ML with a resolution of 1600x1200 pixels and a 8bits per channel. Even it had three available channels they was combined to finally get a single grayscale channel.

By using the function *Sweep,* the application founds itself the optimum position for the translation stage. Then, it was necessary to adjust manually the mirrors M3 and M7 (see figure 5) to reach the best interaction possible. By using the translation stage controls we moved it 1 mm to get out of interaction to capture the background. With this, the application builds the beam model and computes $\tau(x)$. Finally deduces the most suitable chirp curve and give us the pulse duration $\tau(0)$. The experiment was repeated several times and gave us pulse duration from 171fs to 181fs an chirps from 0.25nm/fs to 0.5 nm/fs.

Additionally, in the same conditions, we have done another set of tests in which we have introduced a thick block of crystal just before the setup with the purpose of distort the laser pulse introducing chirp. In this case we obtained a higher pulse duration as well as higher chirp. Specifically, the measured duration was in the range of 190fs to 201fs an the chirp from 0.75nm/fs to 1nm/fs.

Conclusions

We have built and implement a novel auto-correlation technique for ultrashort laser pulse characterization based on the process of transverse SHG in disordered nonlinear crystals. Unlike other well-known auto correlation schemes, our technique may be implemented for the temporal characterization of pulses over a very wide dynamic range (30fs - 1ps) and wavelengths (800 - 2200nm), using the same device and without critical angular or temperature alignment. This device allows a partial characterization of ultra-short pulses measuring the pulse duration and chirp parameter. A special effort has been done to build a compact and automatized set-up, downsizing the setup to finally get a relatively portable device that allow us to easily install and running to take measures on any lab. The software has been designed to be easy to use and reliable allowing to abstract the user of the complexity of the image manipulation and the data processing. Since the software gives you results continuously every second it gives you the opportunity to

perform experiments in where you can change dynamically the input pulse shape and see on-line its changes in relation to duration and chirp. This development could be and start point for the creation of a commercial product that can compete with other similar products currently available in the market. The simple implementation of the set-up allows real-time control of the pulse duration and chirp content at any desired position within an experimental setup.

References

[1] B. E. Saleh and M. C. Teich, Fundamentals of photonics, Wiley New York, 1991.

[2] Characterization of femtosecond pulses via transverse second-harmonic generation in random nonlinear media J. Trull · S. Saltiel · V. Roppo · C. Cojocaru · D. Dumay · W. Krolikowski · D.N. Neshev · R. Vilaseca · K. Staliunas · Y.S. Kivshar

[3] Nonlinear frequency conversion under general phase mismatched conditions: the role of phase locking and random nonlinear domains. Vito Roppo

[4] Ultrashort pulse chirp measurement via transverse second-harmonic generation in SBN crystal J. Trull , I. Sola , B. Wang , A. Parra , W. Krolikowski, Y. Sheng , R. Vilaseca and C. Cojocaru

[5] Characterization of femtosecond pulses via transverse second-harmonic generation in random nonlinear media J. Trull · S. Saltiel · V. Roppo · C. Cojocaru · D. Dumay · W. Krolikowski · D.N. Neshev · R. Vilaseca · K. Staliunas · Y.S. Kivshar

[6] Transverse single-shot cross-correlation scheme for laser pulse temporal measurement via planar second harmonic generation B. Wang (王炳霞), C. Cojocaru, W. Krolikowski, Y. Sheng and J.Trull

[7] Alonso, I. J. Sola, O' . Varela, J. Hernandez-Toro, C. Mendez, J. San Rom'an, A. Za€ır,

and L. Roso, J. Opt. Soc. Am. B 27, 933 (2010)

[8] Bowlan, P. Gabolde, A. Shreenath, K. McGresham, R. Trebino, and S.Akturk, Opt.

Express 14, 11892 (2006)

[9] J. J. Romero, C. Arago, J. A. Gonzalo, D. Jaque, and J. Garcia Sole, "Spectral and

thermal properties of quasi- phase-matchingsecond-harmonic generation in Nd3+

:Sr0.6Ba0.4 (NbO3)2 multi-self-frequency-converter nonlin- ear crystals," J. Appl.

Phys. 93, 3111-3113 (2003)

[10] P. Molina, M. O. Ramirez, and L. E. Bausa, "Strontium Barium Niobate as a

Multifunctional Two-Dimensional Nonlinear "Photonic Glass,"" Adv. Funct. Mat. 18,

709-715 (2008)

[11] M. O. Ramirez, D. Jaque, L. Ivleva, and L. E. Bausa, "Evaluation of ytterbium doped

strontium barium niobate as a potential tunable laser crystal in the visible," J. Appl.

Phys. 95, 6185-6191 (2004)

[12] Vito Roppo, David Dumay, Jose Trull, Crina Cojocaru, Solomon M. Saltiel, Kestutis Staliunas, Ramon Vilaseca, Dragomir N. Neshev, Wieslaw Krolikowski, and Yuri S. Kivshar "Planar second-harmonic generation with noncollinear pumps in disordered media" (2008)

[13] J. Trull, I. Sola, B. Wang, A. Parra, W. Krolikowski, Y. Sheng, R. Vilaseca, and C. Cojocaru "Ultrashort pulse chirp measurement via transverse second-harmonic generation in strontium barium niobate crystal" (2015)